

Re-dating of Chinese celadon shards excavated on Mapungubwe Hill, a 13th century Iron Age site in South Africa, using Raman spectroscopy, XRF and XRD

Linda C. Prinsloo,^{1*} Nigel Wood,² Maggi Loubser,³ Sabine M. C. Verryn³ and Sian Tiley⁴

¹ Department of Physics, University of Pretoria, Pretoria 0002, South Africa

² Research Laboratory for Archaeology and the History of Art, Oxford University, 6 Keble Road, Oxford OX1 3QJ, UK

³ XRF and XRD Laboratory, University of Pretoria, Pretoria 0002, South Africa

⁴ Mapungubwe Museum, University of Pretoria, Pretoria 0002, South Africa

Received 10 January 2005; Accepted 17 March 2005

Chinese celadon shards of the Longquan type, believed to date from the Southern Song dynasty (1127–1279 AD), were excavated in 1934 on Mapungubwe Hill, a 13th century Iron Age site in the Limpopo valley, South Africa. We studied the shards with Raman spectroscopy, x-ray fluorescence (XRF) spectroscopy and x-ray diffraction (XRD). The Raman polymerization index (I_p), calculated from the spectra of the glaze of the shards, indicated a higher firing temperature than expected for the relatively calcium-rich Longquan glazes of the Southern Song dynasty. XRF analysis of the glaze and XRD measurements of the bulk of the shards supported this view and date the shards to possibly the Yuan (1279–1368 AD) or even early Ming (1368–1644 AD) dynasties. These results have an impact on the chronology of the history of the region and therefore call for further research of a comparative nature of other Chinese celadon shards excavated on archaeological sites in Africa, in addition to additional carbon dates of Mapungubwe hill. Copyright © 2005 John Wiley & Sons, Ltd.

KEYWORDS: XRF; XRD; celadon; glaze

INTRODUCTION

The *Illustrated London News* reported on 8 April 1933, 'a remarkable discovery in the Transvaal: a grave of unknown origin, containing much gold-work, found on the summit of a natural rock stronghold in a wild region'.¹

This discovery turned the myths and legends surrounding the sacred hill Mapungubwe (TsiVenda for 'the hill of the jackal') into factual history. An ancient legend, suggesting certain death upon ascending the hill, helped to protect the last resting place of the rulers of a prehistoric African trade kingdom (ca 1000–1290 AD) for more than seven centuries. Furthermore, the occurrence of malaria and tsetse fly made the Limpopo valley the wildest and most desolate part of the Transvaal and helped to protect the site from looting, which occurred at most other Iron Age sites in southern Africa.² The discovery in 1933 of intact gold-bearing graves by prospectors was therefore a remarkable find of great archaeological

and historical significance and marked the beginning of a 70-year archaeological project, which has recently resulted in the founding of the Mapungubwe Museum, University of Pretoria.

Two fragments of Chinese porcellaneous ware were excavated in 1934, during the first archaeological expedition to Mapungubwe, in the occupation layers on the hilltop, one at 4 ft and the other at 1 ft from the surface. They were classified in the same year by the British Museum as celadon from the late Southern Song dynasty (1127–1279 AD).² In 1991, another shard, belonging to the same vessel, was found at the main entrance to Mapungubwe hill.³ The shards and thousands of imported glass beads, which were also excavated at the site, connect Mapungubwe to the extensive maritime trade network, established already in the 1st century AD, which linked East Africa with the monsoon-based commercial systems of the Indian Ocean (Fig. 1). African raw materials such as gold, rhinoceros horn, ivory, ambergris, frankincense and myrrh were exchanged for cotton, porcelain and glass trade beads.⁴

*Correspondence to: Linda C. Prinsloo, Department of Physics, University of Pretoria, Pretoria 0002, South Africa.
E-mail: linda.prinsloo@up.ac.za

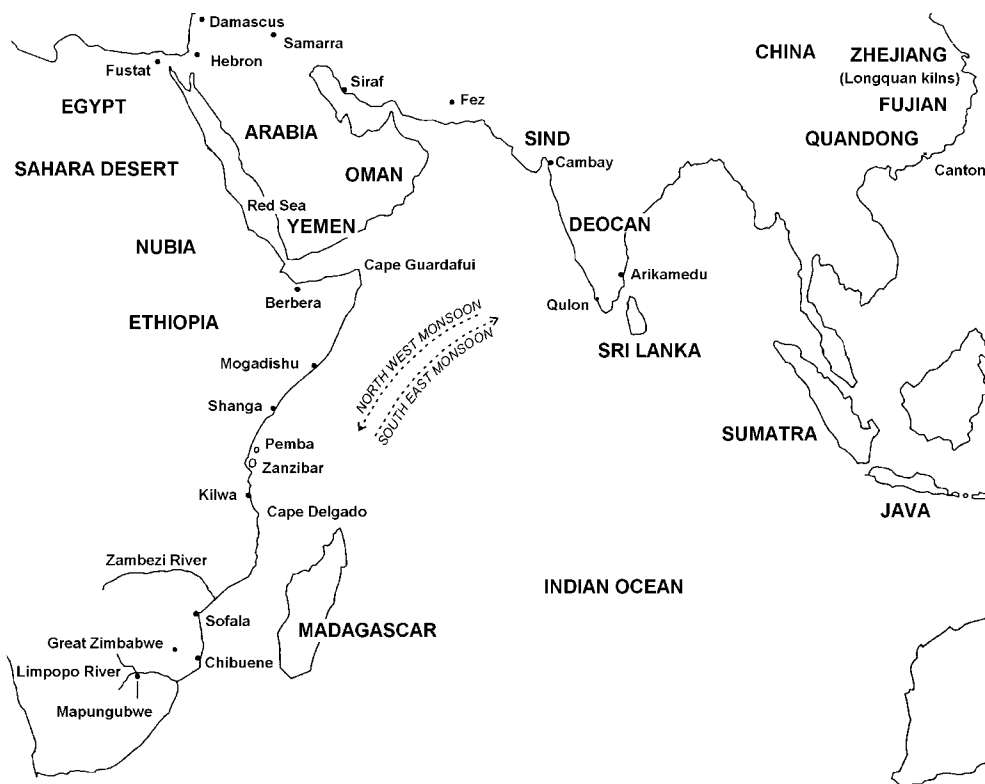


Figure 1. Map depicting Mapungubwe and Great Zimbabwe in geographical context with the important ports and cities of the Islamic trade in the Indian Ocean.

Imported porcelain, stoneware and glass shards have been found at many excavated sites along the East African Swahili coast, such as the Islamic towns of Manda, Shanga and Gedi on the Kenyan coast and the ruins of the Islamic mosque Malindi on the trade island of Kilwa off the east coast of Tanzania. At all of these sites Chinese ceramic shards were found, together with Islamic wares imported from Iran, Persia and India.^{4–11} Exotic imports, when found in a secondary archaeological context, have always provided a basic archaeological dating method if securely dated at their point of origin. In East Africa, it is of cardinal importance as the only written records of the pre-Portuguese era is the Greek *Periplus Maris Erythraei* (~2 AD), a few travel documents from famous Arab travellers such as Al-Masudi and Ibn Battuta (10th century) and hearsay knowledge documented in Chinese sources.⁴ Numerous scholars have used particular varieties of Chinese pottery to refine chronology on the East African coast.^{4–11}

Chinese ceramic shards have also been found at inland ancient Iron Age ruins, all of which are situated in a region spanning Zimbabwe, Zambia and the northern part of South Africa, where ancient pre-European gold, copper and tin mines occurred.² The known imported ceramics recovered from central African Iron Age sites amount to some 100 shards, of which over 90% come from Great Zimbabwe and are nearly exclusively celadon wares, which broadly dates

the shards to pre-Portuguese times.⁸ The porcelains traded by the Portuguese, who replaced the Islamic trade along the east coast after 1498, are largely Chinese blue-and-white porcelains and stonewares and were mostly excavated at established Portuguese trading posts.⁸

In 1934, R. L. Hobson of the British Museum ambiguously dated the shards excavated at Mapungubwe, the most southern ancient ruin where Chinese ceramic ware was found, as celadon from the ‘late Southern Song dynasty, 13th to 14th century’ (see Table 1).^{2,8} He also dated the shards excavated at Great Zimbabwe as Southern Song, but other oriental scholars superseded his classification and agreed that most of the Zimbabwe celadons are Ming.⁸ Classifications at this time were done on a subjective basis

Table 1. The time period of the dynasties of China mentioned in the text

Chinese dynasty	Period
Five Dynasties period	907–960 AD
Northern Song	960–1127 AD
Southern Song	1127–1279 AD
Yuan	1279–1368 AD
Ming	1368–1644 AD
Qing	1644–1911 AD

and relied solely on slight colour variations, shapes and decorations.¹² It was generally assumed, though, that the origin of the shards is the famous Longquan (a district of southern Zhejiang) kilns, where the production of celadons reached their peak in the 13th and 14th centuries, when they were exported widely to Japan, East Africa, the Philippines and the Near East.

Renewed interest in Mapungubwe and the prehistory of South Africa instigated this study and we used Raman spectroscopy, x-ray fluorescence (XRF) spectroscopy and x-ray powder diffraction (XRD) to analyse the chemical composition of the shards in an attempt to determine their provenance and production date with greater accuracy and objectivity than before.

EXPERIMENTAL

Samples

The two shards (Acc. No. N/193) originally excavated on Mapungubwe hill in 1934 can be seen in Fig. 2a. There are three shards in the photograph as the smallest fragment has unfortunately broken off one of the shards through the years, but it can be seen that the shards originally belonged to one vessel (fourth shard found in 1991 not shown). The distinctive ribbed pattern, known as melon ridge, was popular in both northern and southern ancient China. It appears as if two 'bowls', originally moulded, were made and joined rim to rim (maybe off the wheel) and the inside of the shard clearly shows where the two pieces have been attached [Plate 1(c)]. The beautiful green glaze, typical of Chinese celadon ware, and the fine quality of the ceramic survived the harsh African weathering conditions remarkably well and is silent testimony to an ancient potter's craft.

The shards were ultrasonically cleaned to eliminate fluorescence from organic material, which could have adhered to the sample before excavation, by handling or contamination with naphthalene, which in the past was commonly used as a preservative in museum collections.

The original classification of the shards as Southern Song was supported by a study in which the fragments were visually compared with a Chinese celadon spouted vessel, from the Van Tilburg Collection, University of Pretoria (J. A. van Tilburg, a Dutch collector, emigrated in 1952 to South Africa and donated the collection to the University. The collection contains 3000 pieces of Chinese ceramic ware of high quality with representative pieces dating from the Chin to the Qing dynasty). The official museum description of the vessel is Longquan celadon from the Southern Song dynasty [Plate 1(b)]. The colour, texture of the ceramic, unique form and ribbed pattern were found to be so similar that it was positively stated that the potshard originated from a comparable object (referred to in the article as wine kettle).¹³ However, Regina Krahl, independent scholar and a current expert on Chinese ceramics at Sotheby's, London, suggests

that the shards may derive from a moulded jar or bowl of similar style, which tend to have deeper ribs than this type of ewer (R. Krahl, personal communication). We included the spouted vessel in our study for comparative reasons.

Techniques

Raman spectroscopy

Raman spectra were recorded with an XY Raman spectrometer from Dilor, using both 514.5 and 488 nm radiation from a Coherent Innova 90 argon ion-laser for excitation. The excitation powers at the samples were kept below 20 mW to avoid any thermal effects and the slit width was adjusted to obtain a resolution of at least 2 cm⁻¹. The 50× and 100× objectives were used in a backscattering configuration to collect spectra of the glaze and body of the samples.

The size of the confocal hole, magnification of the objectives and laser power were varied to obtain the optimum recording conditions at each sampling spot. At least 20 spectra were recorded from each phase to obtain statistically representative data. Spectra recorded on the spouted vessel were limited to specific spots owing to the bulkiness of the object, which could be placed in only a few positions underneath the microscope.

In the case of the shard, spectra of the glaze could also be recorded on the side of the fragment, as the glaze between indentations on the shard is fairly thick [Plate 1(c)].

Peak fitting and data processing

In the spectra used for curve fitting, the baseline was first subtracted with a polynomial fitting of x^3 or x^4 using Labspec (Dilor) software. The number of attach points was minimized and kept constant for attaching the baseline to the different spectra. A Gaussian shape was assumed and the same spectral window used for extraction of the components, using the Origin peak-fitting module. The methods applied by Colomban and co-workers in their extensive work on porcelain were followed as closely as possible in order to compare the results obtained in this study with the graphs generated by their group. The integral under each component envelope was also calculated with the Labspec software.

XRD

XRD data were collected from both the bulk and the glaze of the smallest shard on a Siemens D501 automated diffractometer equipped with a secondary graphite monochromator. The applied potential was 40 kV and the corresponding current was 40 mA. The primary x-ray beam was Cu K α radiation. A pattern was recorded from 3 to 70° 2 θ in steps of 0.04° 2 θ . The measuring time was 1 s per step.

XRF

Two of the celadon shards were analysed using XRF spectroscopy. They were directly mounted in a 90° quadrant of a Perspex ring and introduced to an ARL 9400XP+ wavelength-dispersive (WD) XRF spectrometer. Analyses

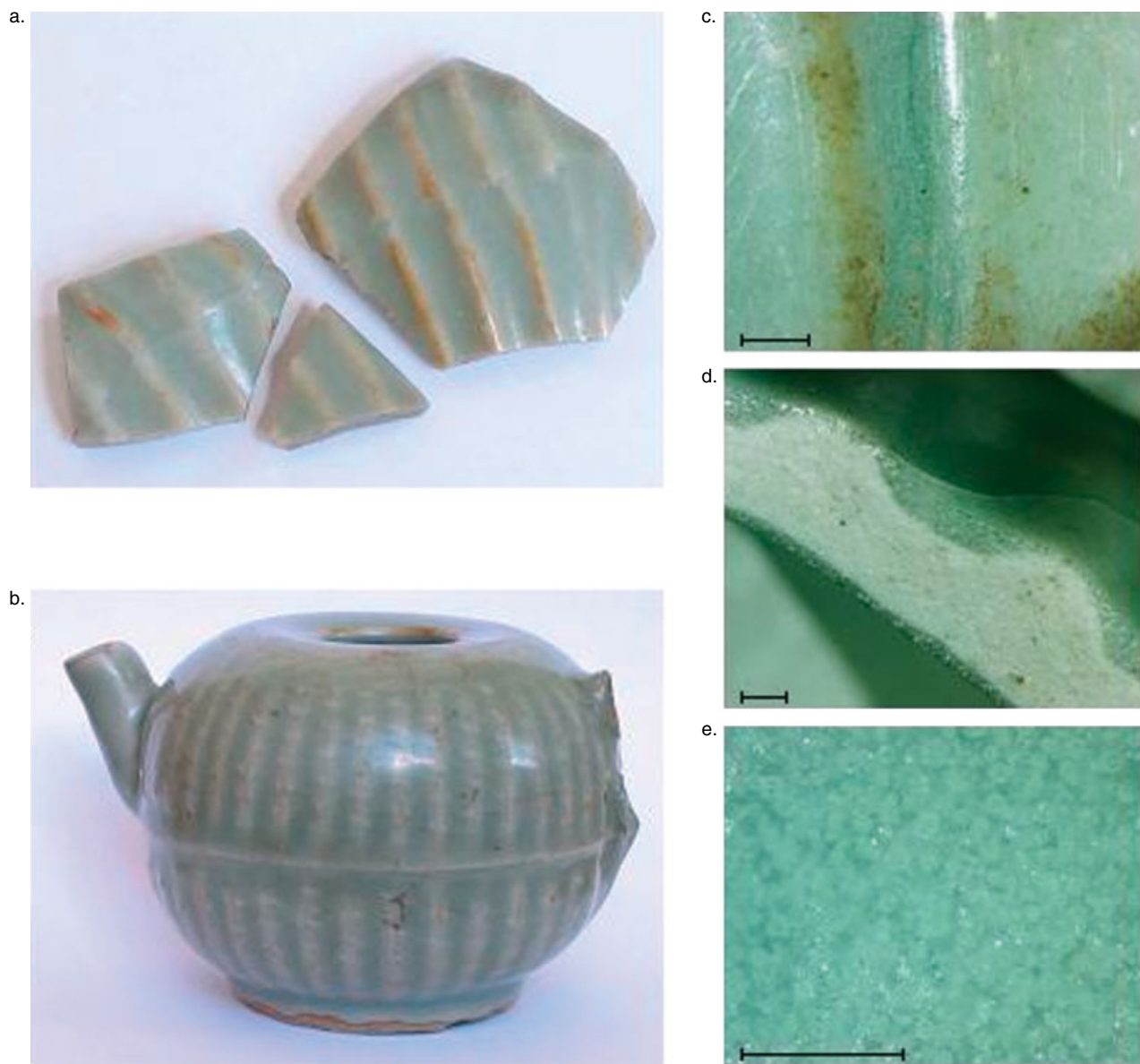


Plate 1. (a) Celadon potshards excavated on Mapungubwe hill. (b) Spouted vessel classified as Southern Song celadon. (c) Back side of a shard showing where two halves of the vessel have been joined. (d) Side view of shard. (e) Close up of shard glaze. Bar = 1 mm in (c)–(e).

Table 2. Analytical conditions used over the entire range for XRF measurements

Crystal	2d crystal/Å	Collimator divergence/°	Detector	X-ray tube anode	Tube setting		Primary beam filter
					kV	mA	
LiF220	2.8480	0.15	Scintillation	Rh	60	40	0.25Cu
LiF420	1.8000	0.15	Scintillation	Rh	60	40	
LiF220	2.8480	0.15	Flow proportional	Rh	40	60	
GE111	6.5320	0.15	Flow proportional	Rh	40	60	
AX06	55.400	0.60	Flow proportional	Rh	30	80	

were executed using the UniQuant 5 software program, specifying the weight and area of sample. The software analyses for all elements between F and U and only elements above the detection limits are reported. The spectrometer conditions used over the entire analytical range are displayed in Table 2.

Historically, energy-dispersive (ED) XRF spectroscopy was used for the analysis of porcelains because most WDXRF background and matrix correction software packages assume homogeneous, infinitely thick, flat specimens. The UniQuant 5 software program differs in this regard in that the author included in his algorithms factors to compensate for non-infinitely thick, irregularly shaped and small samples. This enables the analyst to use WDXRF in the same manner as EDXRF that historically had better matrix correction software, owing to the complexity of deconvoluting peaks in EDXRF.

RESULTS AND DISCUSSION

Raman spectroscopy

Raman spectroscopy has been used successfully to study the bulk material, glazes and pigments from a great variety of art objects such as porcelain, glass, jewellery, mosaics and pottery. It has proved to be extremely useful in determining the kind of pigments used, to distinguish between hard-paste and soft-paste porcelains, to differentiate between ancient and modern porcelain and to make deductions about the technology used in manufacturing processes.^{14–27}

Raman spectra of the bulk material

The dense, pale-grey body of the shard is typical of Longquan celadon ware, which is considered in China as a type of porcelain. Indeed, it is far closer to white porcelain in its chemical composition than to any stoneware (including celadon) made in any other part of China.²⁸ Spectra of the bulk of the shard could be recorded through the glaze, in addition to directly on the bulk from the side, and in Fig. 2 representative spectra recorded on the bulk of the shard are presented.

In most spectra, the strong characteristic peak at 462 cm⁻¹ of α-quartz was detected (not shown), which is expected of a silica-rich body. This is in accordance with the raw materials used in south Chinese high-fired ceramics, which

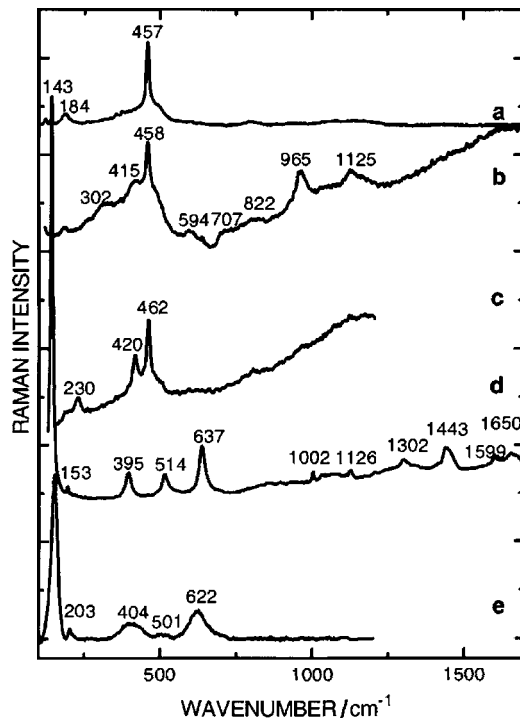


Figure 2. Spectra recorded on the bulk of the shard: (a) glassy silica and α-quartz; (b) glassy silica, α-quartz and mullite; (c) cristobalite; (d) anatase and organic phase; (e) anatase to rutile transition phase.

consisted of igneous rocky materials that were originally molten rock (magma). These materials were, in contrast to Northern Chinese raw materials, low in ‘true clay’ minerals such as kaolinite and consist instead largely of fine α-quartz and secondary potassium mica, which makes the ceramics rich in silicon and potassium oxides and relatively low in aluminium oxide.²⁹

In spectra recorded of the body through the glaze or recorded in the interface region between body and glaze from the side, this peak occurs at 457 cm⁻¹ [Fig 2(a)]. The shift of the peak from 464 cm⁻¹ in pure SiO₂ to lower wavenumbers (457–460 cm⁻¹) has been attributed to tensile stress, which exists in small grains of quartz in the interface layer.¹⁹ It should be noted, however, that we observed this shift also in

spectra not recorded on the interface but always in association with the peak at 450 cm^{-1} , characteristic of silica glass, as also seen in the spectrum in Fig. 2(b) discussed below.

The spectrum in Fig. 2(b) represents a mixture of typical phases of the crystalline and glassy phases of the silica–alumina system. The peak at 458 cm^{-1} , as already mentioned, is crystalline α -quartz superimposed on the broad band around 450 cm^{-1} typical of glassy silica. The broad peaks at 302 , 415 , 960 and 1104 cm^{-1} are typical of polycrystalline mullite, one of the expected phases in well-fired porcelain.³⁰

The two peaks at 230 and 420 cm^{-1} observed in Fig. 2(c) (recorded on the interface between the bulk and the glaze) are typical of cristobalite, a high-temperature polymorph of SiO_2 . The development of cristobalite requires heat treatment for a long duration, which typically occurred in old ceramic kilns.²⁰ 'Dragon kilns', of the type used for Longquan wares, were first developed by potters in south China in the Shang dynasty (16–11th centuries BC) and refined in subsequent centuries. They consist of long tunnels built on the slope of a hill, with later examples fired by both large fireboxes at the feet of the tunnels, and by side stoking along the kilns' lengths. They reached their zenith in the early 12th century AD when an example approaching 140 m was built in Fujian province. This was capable of firing 10^5 vessels in a single setting. Longquan kilns were somewhat shorter, but would still have provided suitable conditions for the formation of cristobalite.³¹

Peaks at 143 , 197 , 399 , 513 and 639 cm^{-1} originate from the anatase phase of TiO_2 [Fig. 2(d)] and were observed in many of the spectra recorded on the bulk and also the glaze of the shard. TiO_2 is present (0.2–2.0%) in most Chinese ceramic raw materials and its relative ratio with respect to iron oxides helps determine the shade of green in celadon glazes when fired in a reducing atmosphere.²⁸ The very large Raman cross-section of TiO_2 phases makes even these relatively small percentages easy to detect. In the same spectrum [Fig. 2(d)], peaks between 1000 and 1700 cm^{-1} are also observed and are attributed to carbonaceous and organic phases, which have previously also been observed in ceramic glazes. These residues arise from firing in a reducing atmosphere and from contamination, respectively.¹⁸

In some of the spectra, the characteristic anatase high-intensity peak at 143 cm^{-1} occurs at 153 cm^{-1} , as seen in Fig. 2(e). The relative intensity of the peak has also decreased in these spectra and the FWHM increased from 6 to 15 cm^{-1} . Simultaneously, the other peaks broadened and shifted slightly to 203 , 403 , 504 and 623 cm^{-1} with the appearance of a new small peak at 285 cm^{-1} . It is well known that three polymorphs of TiO_2 exist in nature, namely the stable rutile phase and the metastable anatase and brookite phases, which convert to rutile on heating. Brookite converts directly to rutile, whereas anatase can convert directly or via brookite to rutile. The temperature of the anatase–rutile phase transformation is furthermore influenced by the size of

the particles, the presence of other minerals and the amount of brookite present, and has been extensively studied.^{32–36} Although pure brookite has a strong peak at 153 cm^{-1} , the other strong peaks associated with the brookite phase at 245 , 320 , 364 and 449 cm^{-1} are absent in the spectra, so it is assumed that the observed spectrum is a transition phase between anatase \rightarrow brookite \rightarrow rutile. The firing temperature was therefore not high enough to cause a complete transformation to the rutile phase under these specific conditions. It has been recorded that this peak occurs at 153 cm^{-1} for nanosized anatase particles, which could be another explanation for the shift, but as it is known that the porcelain had been heated to at least 1200°C , the former explanation is more likely.

The body of the spouted vessel could be analysed on the bottom rim, where the glaze had not been applied. Similarly to the body of the shard, in some spectra only crystalline α -quartz [Fig. 3(a)] with the most prominent peak at 462 cm^{-1} was observed. In most spectra both glassy alumina silicate with its broad band around 450 cm^{-1} and crystalline α -quartz are clearly observed [Fig. 3(b)]. Spectra of TiO_2 in the rutile phase with bands at 144 , 246 , 441 and 605 cm^{-1} were also recorded and are an indication that the body of the spouted vessel was fired at a higher temperature than the shard, as the phase transformation to rutile has taken place [Fig. 3(c)]. The relative intensity of the 143 cm^{-1} band, with FWHM equal to $\sim 10\text{ cm}^{-1}$, is an indication that there is still anatase present, as in pure rutile samples the relative intensity of this band is significantly decreased, with an FWHM of $\sim 3\text{ cm}^{-1}$. The sharp peak at 1084 cm^{-1} in the rutile spectrum is the characteristic C–O stretch vibration of calcium carbonate.

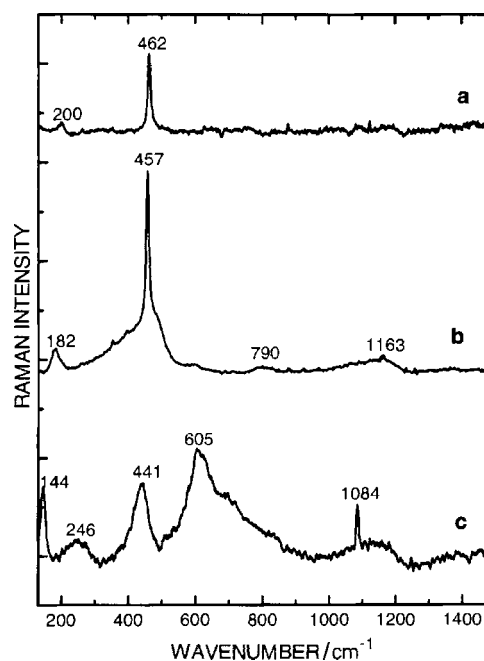


Figure 3. Spectra recorded on the bulk of the spouted vessel: (a) α -quartz; (b) glassy silica and α -quartz; (c) rutile.

CaCO₃ breaks down during firing at about 800 °C, liberates carbon dioxide and converts to CaO. Therefore, it is probably contamination, which occurred after firing.

Raman analysis of the body of both the shard and spouted vessel is in agreement with the silica-rich composition of Southern Song celadon bodies from the Longquan kilns. The presence of rutile in the body of the vessel indicates that the firing temperature of the bulk of the teapot was probably higher than for the shard.

Raman spectra of the glaze

Small white particles and micron-sized bubbles suspended in the glaze could be distinguished under the microscope [Plate 1(e)] and made it possible to record a spectrum of α -quartz on a specific particle with the 100 \times objective (not shown). The α -quartz crystallites and bubbles suspended in the glaze (also observed in Vietnamese celadon²³) are typical of celadon glazes and, together with the formation of anorthite and wollastonite crystals in the glaze, responsible for their jade-like texture.^{28,31}

A glaze is a dense alumina–silicate glassy phase doped or mixed with other metallic oxides, which act as flux to lower the temperature of the glass transition. The addition of metallic cations breaks the Si–O linkages, which decreases the degree of polymerization in the Si–O network and consequently requires a lower firing temperature.

The Raman spectra of porcelain glazes consist of two broad bands around 500 and 1000 cm⁻¹. The band around 500 cm⁻¹ originates from the ν_2 bending vibration of isolated SiO₄ tetrahedra and that around 1000 cm⁻¹ to coupled ν_1 and ν_3 Si–O stretching vibrations.¹⁹ In highly connected tetrahedral structures the bending modes have a high Raman intensity and in weakly connected tetrahedral units, as caused by the addition of fluxing agents, the intensity of this band decreases and the stretching modes become more intense. The relationship between the Raman index of polymerization ($I_p = A_{500}/A_{1000}$, where A is the area under the Raman band), the glass composition and the processing temperature are well documented.^{21–27}

In the Raman spectrum of the glaze of the Mapungubwe shard [Fig. 4(a)], the first peak around 500 cm⁻¹ is obviously more intense than the peak around 1000 cm⁻¹ and indicates a highly connected structure of SiO₄ tetrahedra. The average value of $I_p = 1.6$ for the glaze of the Mapungubwe shard places it in the same category as Vietnamese porcelain glazes, which according to the graphs in Refs 21–27 is a phase between Vietnamese calcium rich celadon glazes, with $I_p \approx 1.2$, and hard-paste porcelain glazes ($2.7 < I_p < 7$). It has been shown that the composition of Chinese Southern Song celadon glazes is very similar to that of their Vietnamese counterparts and in both cases CaO (~10%) was used as chief fluxing agent. Although exceptions are, of course, possible it would seem that the Mapungubwe shard's index of polymerization does not exactly match that of the relatively Ca-rich ancient Vietnamese (or Southern Song) glazes, but

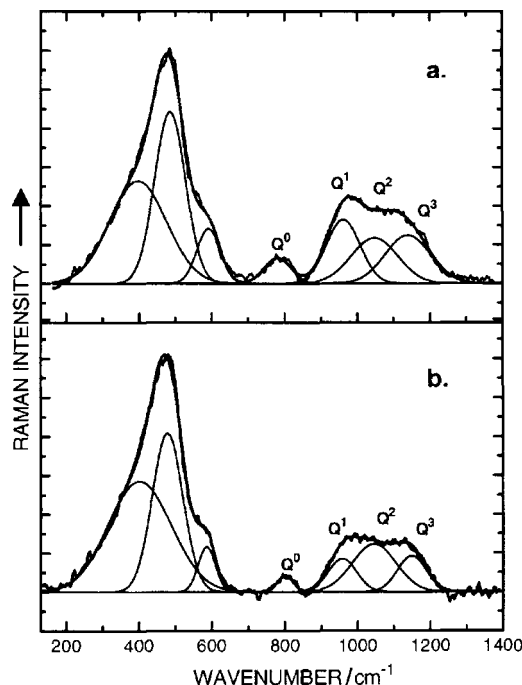


Figure 4. Spectra recorded of the glaze: (a) shard; (b) spouted vessel.

rather a transition stage between glazes with Ca as main fluxing agent and feldspathic glazes with potassium as chief fluxing agent. Parallel evolution in time to glazes relatively richer in K₂O + Na₂O and lower in CaO occurred in both China and Vietnam.

Spectra recorded of the glaze of the spouted vessel [Fig. 4(b)] are very similar to that obtained for the shards and have an average $I_p = 2.6$, which is just below the I_p of modern hard-paste porcelain glazes.

The different components of the stretching envelope of porcelain glazes were assigned in the literature to silica vibrations with zero (Q⁰ or isolated SiO₄, ca 800–850 cm⁻¹), one (Q¹ or Si₂O₇ groups, ca 950 cm⁻¹), two (Q² or silicate chains), three (Q³ or sheet-like region, ca 1100 cm⁻¹) and four (Q⁴, SiO₂ and tectosilicates, ca 1150–1250 cm⁻¹) bridging oxygens per tetrahedral group. We did not differentiate between Q³ and Q⁴ components and the positions of the deconvoluted peaks of the glaze spectra of the shard and the spouted vessel are compared in Table 3. The positions conform to the expected values for silica-based glazes. Q¹ has the highest intensity in the glaze of the shard [Fig. 4(a)] with

Table 3. Positions of the components (wavenumbers/cm⁻¹) of the stretching envelope in the Raman spectra of the glazes of the shard and spouted vessel

	Q ⁰	Q ¹	Q ²	Q ³ –Q ⁴
Mapungubwe shard	780	961	1047	1139
Teapot	800	957	1045	1148

Q^3 – Q^4 the least intense and in this resembles that of Ca-rich celadon glazes of Vietnam. In the stretching envelope of the glaze of the spouted vessel Q^2 is the most intense component [Fig. 4(b)], which is also the case for the glazes of modern hard paste porcelains. The Q^1 and Q^3 – Q^4 components are slightly more intense than for the modern high-temperature glazes and this result is supportive of the classification of the glaze as an intermediate composition between Vietnamese Ca-rich celadon glaze and K-feldspar glaze fired at higher temperatures.

The Raman spectra recorded of the glazes of the Mapungubwe shard and the spouted vessel classified it as belonging to a family of glazes between Ca-rich glazes and glazes of modern hard-paste porcelains. It indicates that both the shard and spouted vessel may have been manufactured at a later stage than their official museum classifications. This result motivated us to also analyse the shard with other analytical methods, namely XRD and XRF spectroscopy.

XRD

XRD measurements are supportive to the information obtained with Raman spectroscopy, as it also gives an indication of the relative quantity of a specific phase present within a material. Only the shard could be studied owing to size restrictions of the sample holder. Glassy (amorphous) phases cannot be identified by XRD and therefore, although the glaze was analysed, no usable results were obtained.

In Fig. 5 the diffraction pattern of the body of the shard is presented. The peaks of the main components are indicated as α -quartz (Q) and mullite (M). The mullite peaks largely overlap with those of sillimanite, a precursor to the formation

of mullite. Raman data, however, confirmed the presence of mullite and therefore only mullite peaks are indicated in Fig. 5. The ratio of the highest mullite peak ($d = 3.39 \text{ \AA}$) to the most intense peak of quartz ($d = 3.34 \text{ \AA}$) is 0.26 and resembles that attributed to porcelain of the Qing dynasty produced in Jingdezhen.³⁷ The small percentage of mullite present is supportive of the fact that the shards originate from southern China, rather than northern China, as the raw materials used in northern China were rich in kaolin and would result in higher percentages of mullite.³⁸

Traces of corundum, K-feldspar, plagioclase feldspar and iron may be present, as indicated in Fig. 5. All of these minerals are typical of Chinese raw materials and support the Chinese origin of the celadon. The elemental iron detected is in accordance with the greyish tone of the body.

XRF spectroscopy

XRF has become one of the major techniques used in the study of porcelain, as it non-destructively determines the percentage of the major oxides present in the porcelain body and glaze.^{39–41}

The spouted vessel could not be analysed with our current experimental setup. In Table 4, the main oxide compositions of two of the Mapungubwe shards are compared with those of the Longquan celadon glazes originating from the Five Dynasties to the Ming period.²⁸ The small difference in quantitative analyses on the two Mapungubwe shards could be ascribed to different orientations of the pieces in the spectrometer and thus more of the porcelain body analysed in the one and more glaze in the other. The Uniquant 5 software includes algorithms for irregularly shaped or small

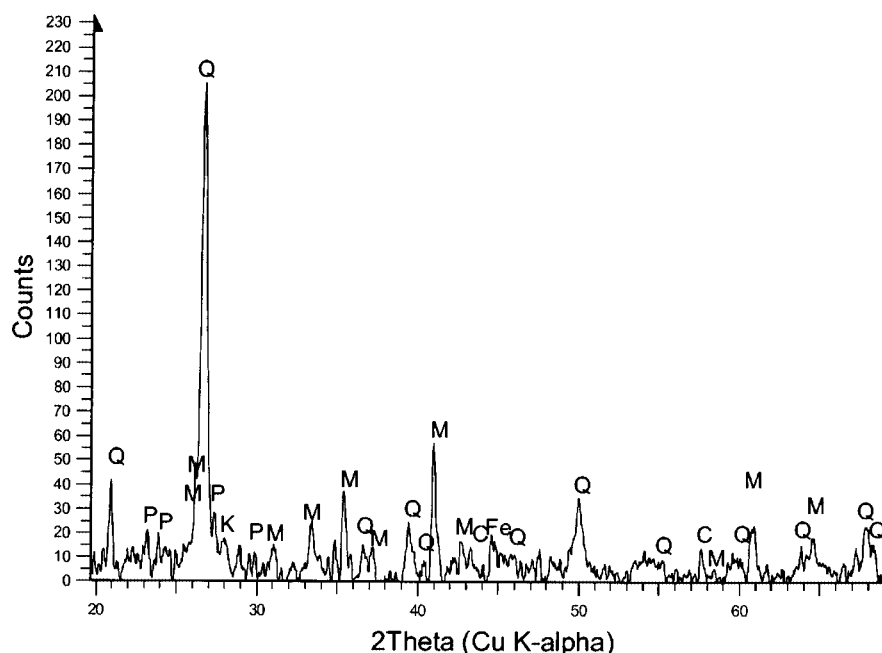


Figure 5. X-ray diffraction trace. Q = quartz, M = mullite, Fe = iron, P = plagioclase feldspar, K = K-feldspar, C = corundum.

Table 4. Comparison of the XRF glaze analysis of the Mapungubwe sample with Longquan celadon glazes (wt%)

	SiO ₂	Al ₂ O ₃	TiO ₂	Fe ₂ O ₃	CaO	MgO	K ₂ O	Na ₂ O	MnO	P ₂ O ₅
Five Dynasties ^a	59.4	16.0	0.4	1.8	16.0	2.0	3.4	0.3	0.6	–
Northern Song ^a	63.2	16.8	0.2	1.4	13.0	1.1	3.3	0.6	0.4	–
Southern Song ^a	68.6	14.3	0.02	0.7	10.4	0.4	5.0	0.1	–	0.14
Yuan ^a	67.4	16.7	0.2	1.5	6.8	0.6	5.5	1.1	0.4	–
Ming ^a	67.6	15.0	0.3	1.4	6.3	1.7	6.5	1.1	–	–
Mapungubwe shard A	67.1	15.7	0.2	2.63	4.37	1.22	6.53	0.82	0.22	0.44
Mapungubwe shard B	68.19	15.72	0.13	2.03	4.48	0.52	6.98	0.994	0.189	0.40

^a Ref. 28.

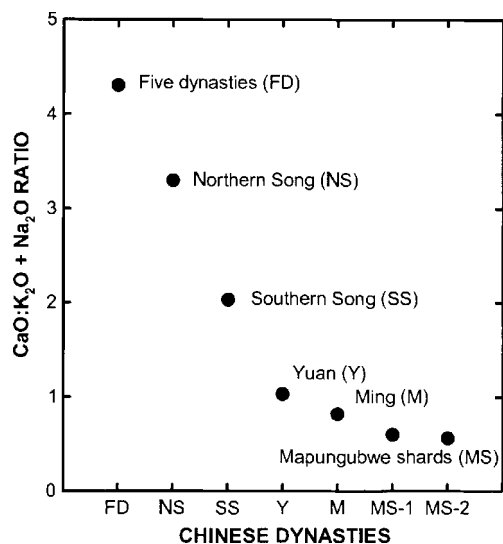


Figure 6. Comparison of the CaO:K₂O ratio of Chinese celadon glazes from Five Dynasties to Ming.

samples, but in some of these cases the samples were irregularly shaped and small and the number of unknowns tested the software’s resolving power. It is obvious that the main oxide composition of the glaze of the Mapungubwe shard closely resembles that of a glaze from the Yuan or early Ming period, rather than that of the Song dynasty (Table 4). The main difference is the CaO:K₂O + Na₂O ratio, which decreased with advancing centuries (Fig. 6), whereas the Al₂O₃ and SiO contents show only small variations (Table 4). A similar evolution (decrease in CaO content) was observed in Vietnamese celadon, but in a smaller time range (12–15th centuries), as illustrated in Fig. 1 of Ref. 20.

The potassium oxide concentration in the glaze is much higher than in hydromica, which was the main source of the potassium oxide in the porcelains of southern China. Chinese researchers believe that the additional potassium was derived from wood ashes fairly rich in potassium oxide and/or from the use of less weathered glaze stones that contained some primary potash feldspar.⁴²

The P₂O₅ content of the glazes examined may suggest the former. The presence of relatively high levels of P₂O₅, MgO and MnO usually shows that plant ash has been part

of the glaze recipe to supply CaO, as plant ash is rich in these compounds whereas limestones and calcium-bearing clays are not.²⁸

Impact on the chronology of the pre-history of southern Africa

The Raman and XRF data suggest that the Mapungubwe shard was possibly manufactured at a later date than previously assumed. This result is extremely important for the chronological history of sub-Saharan Africa as the current opinion is that the last occupation date of Mapungubwe hill is 1280 AD.^{43,44} According to carbon dating of Mapungubwe and Great Zimbabwe, it has been stated that the initial growth of Great Zimbabwe as a major centre can be firmly placed to the third quarter of the 13th century, after Mapungubwe’s decline.⁴³

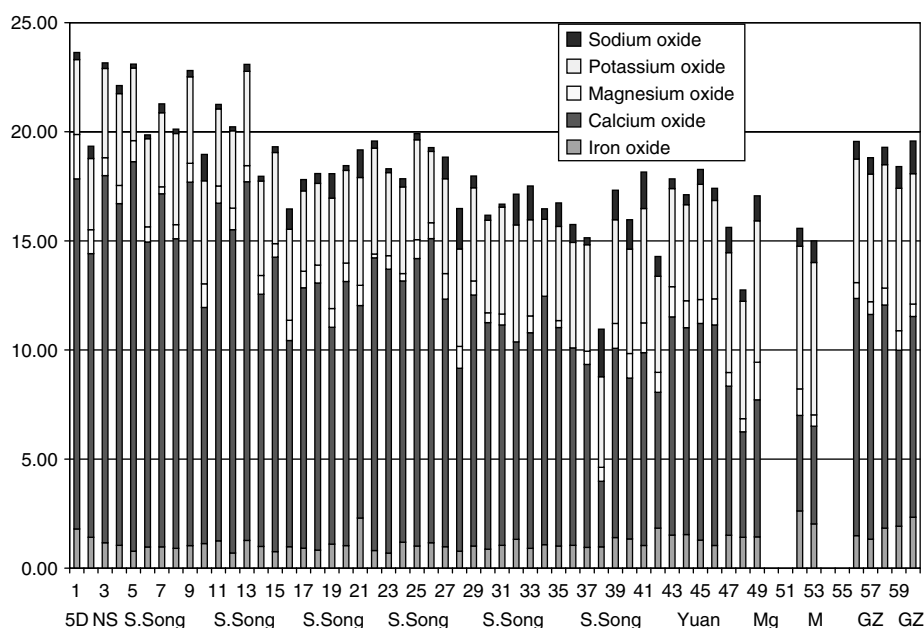
Celadon shards manufactured in the Yuan or early Ming dynasty, buried in the occupation levels on the hill, suggest that the last occupation of Mapungubwe could be later than currently believed.

XRF results from shards excavated at Great Zimbabwe

The results obtained from the Mapungubwe shard motivated us to initiate a study on other shards excavated at related southern African Iron Age sites for comparative purposes. A few celadon shards excavated at Great Zimbabwe (purchased from Hall¹⁰ and presented to the South African Museum in 1894 by the British South African Company) were analysed with XRF and the results are summarized in Table 5. It is clear that there is a difference in CaO:K₂O + Na₂O ratio between these shards and the Mapungubwe shard. Assigning the shards to a specific dynasty is not straightforward. The maturing temperatures of ceramic glazes are dependent on the total of all the oxides used as fluxing agents, in particular the four oxides CaO, MgO, K₂O and Na₂O, which for Longquan celadon glazes are the main fluxing agents. In Fig. 7, the total fluxing contents in Longquan celadon glazes from the Five Dynasties to early Ming⁴⁵ are compared with those of the Mapungubwe and Great Zimbabwe glazes. On this score the Mapungubwe glazes seem higher firing than the Great Zimbabwe shards and much more in the style of the Yuan–Ming range at Longquan. From this view, the Great Zimbabwe shards seem closer to Southern Song examples.

Table 5. Comparison of the XRF glaze analysis of the Mapungubwe sample with the glazes of samples excavated at Great Zimbabwe, (wt%)

	SiO ₂	Al ₂ O ₃	TiO ₂	Fe ₂ O ₃	CaO	MgO	K ₂ O	Na ₂ O	MnO	P ₂ O ₅
Mapungubwe shard A	67.1	15.7	0.2	2.63	4.37	1.22	6.53	0.82	0.22	0.44
Mapungubwe shard B	68.19	15.72	0.13	2.03	4.48	0.52	6.98	0.994	0.189	0.40
Great Zimbabwe 669A	62.01	15.96	0.11	1.49	10.87	0.73	5.66	0.81	0.41	1.17
Great Zimbabwe 669B	64.00	15.58	0.09	1.33	10.30	0.58	5.85	0.75	0.37	0.64
Great Zimbabwe 669C	60.25	17.89	0.15	1.83	10.23	0.78	5.65	0.80	0.63	0.99
Great Zimbabwe 669D	63.28	15.93	0.13	1.92	8.07	0.89	6.53	0.99	0.56	1.11
Great Zimbabwe 7890	64.17	14.19	0.12	2.34	9.19	0.58	5.97	1.50	0.31	0.49

**Figure 7.** Totalled potassium + sodium oxide levels in Longquan celadon glazes (wt%). Five Dynasties to early Ming. Includes Mapungubwe (M) and Great Zimbabwe (GZ) shards.

However, the K₂O + Na₂O levels in the Great Zimbabwe shards are very much of the Yuan–Ming trend, which is more significant (Fig. 8). The high alkali metal content in the Great Zimbabwe shards is more important than their CaO levels, and perhaps indicative of a Yuan–Early Ming production date at Longquan.⁴⁵ This is in contrast to the current literature classification of most of the shards excavated at Great Zimbabwe as entirely Ming.⁸

CONCLUSION

Comparison of the Raman spectra of the glaze of the Mapungubwe shard with literature values made it possible to link the firing temperature and composition of the glaze to a later manufacturing date than previously assumed. In this we illustrated the intrinsic value of the systematic classification of the composition of porcelain glazes according to their Raman spectra undertaken by Colomban and co-workers.

The validity of the Raman analysis was confirmed by the oxide composition of the glaze as determined with XRF spectroscopy. Relating this result to manufacturing processes in ancient China was only possible with the help of recent research on Chinese ceramics, which resulted in accurate databases.^{28,45}

These results suggest that the manufacturing time of the shard may have been the Yuan or early Ming dynasty rather than the Southern Song. Regina Krahl, Chinese ceramic expert, classified the shards according to their appearance as 14th-century Yuan (R. Krahl, personal communication). This too differs from the results of the seven carbon dates obtained from material from Mapungubwe hill, which dates the last occupation of the hill as 1280 AD, and coincides with the end of the Southern Song dynasty.^{39,40} The small sampling size of the carbon dating, and the fact that the calibration curve used in the dating process at this period of time is rather ambiguous, have motivated a project, to be undertaken by

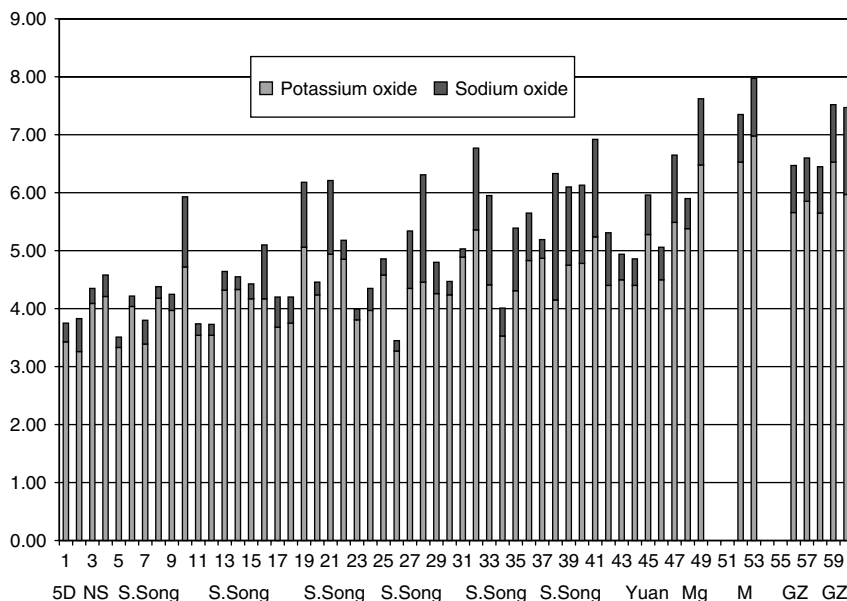


Figure 8. Totalled flux contents in Longquan celadon glazes (wt%). Five Dynasties to early Ming. Includes Mapungubwe (M) and Great Zimbabwe (GZ) shards.

the Quaternary Dating Unit of the CSIR, Pretoria, to obtain additional carbon dates from Mapungubwe hill.

The Raman spectra of the glaze of the spouted vessel suggest that the museum classification might be reconsidered. In the light of the extensive research undertaken since the 1970s at Chinese kiln sites and improvement of non-destructive techniques to analyse museum objects, a project has been initiated to classify all of the objects in the Van Tilburg Collection with more modern methods.

The celadon shards found at Mapungubwe are related to all the imported ceramics excavated at other Iron Age inland sites, and also the African east coast. Therefore, we have initiated a project to study all of these imported ceramics and glass beads with modern analytical methods. The preliminary results from this study, presented in this paper (Table 3), of a few shards excavated at Great Zimbabwe, confirmed that dating the shards with greater accuracy and objectivity would provide supplementary data to obtain a fuller picture of the chronology of trade along the East African coast.

Acknowledgements

The authors thank Iziko Museums of Cape Town (incorporating the South African Museum) for the loan of the shards from their collection. We also thank A. E. Duffey, curator of the van Tilburg, Museum, University of Pretoria (UP), for comments on the manuscript, the Laboratory for Microscopy and Microanalysis, UP, for help with the photographs and the Chemistry Department, UP, for the use of the Raman instrument.

REFERENCES

1. Paver FR. *Illustrated London News* 1933; 8 April: 494.

2. Fouché L. *Mapungubwe: Ancient Bantu Civilization on the Limpopo*. Cambridge University Press: Cambridge, 1937; 1.

3. Meyer A. *The Archeological Sites of Grefswald, Stratigraphy and Chronology of the Sites and a History of Investigations*. V&R Printing Works: Pretoria, 1998; 203.

4. Chittick HN. In *The Peopling of the East African Coast East in Africa and the Orient: Cultural Syntheses in Pre-Colonial Times*, Chittick HN, Rotberg RL (eds). Holmes and Meier Publishers: New York, 1975; 1.

5. Chittick HN. *Kilwa, an Islamic Trading City on the East African Coast. 2. The Finds*. The British Institute in Eastern Africa, Memoir 5. Kenya Litho: Nairobi, 1974; 308.

6. Chittick HN. *Manda, Excavations at an Island Port on the Kenya Coast*. The British Institute in Eastern Africa, Memoir 9. Oxford University Press: Oxford, 1984; 65.

7. Kirkman J. In *Studies in African History*, Stahl KM (ed). Mouton: The Hague, 1963; 45.

8. Garlake PS. *J. Afr. History* 1968; 9(1): 13.

9. Caton Thompson G. *The Zimbabwe Culture: Ruins and Reactions*. Frank Cass: London, 1971; 185.

10. Hall RN. *Pre-historic Rhodesia*. T. Fisher Unwin: London, 1909; 237.

11. Horton M. *Shanga: the Archaeology of a Muslim Trading Community in the Coast of East Africa*. The British Institute in Eastern Africa, Memoir 14. London, 1996; 303.

12. Hobson RL. *Chinese Pottery and Porcelain, an Account of the Potters Art in China from Primitive Times to the Present Day. Vol. 1, Pottery and Early Wares*. Cassell: London, 1915; 76.

13. Meyer A, Esterhuizen V. *S. Afr. J. Ethnol.* 1994; 17(3): 103.

14. Zoppi A, Lufurmento C, Castellucci EM, Migliorini MG. *Spectrosc. Eur.* 2002; 14(5): 17.

15. Sakellariou K, Miliari C, Morresi A, Ombelli M. *J. Raman Spectrosc.* 2004; 35: 61.

16. Colomban Ph, Milande V, Lucas H. *J. Raman Spectrosc.* 2004; 35: 68.

17. Colomban Ph, Treppoz F. *J. Raman Spectrosc.* 2001; 32: 93.

18. Colomban Ph, Sagon G, Faurel X. *J. Raman Spectrosc.* 2001; 32: 351.

19. Liem NQ, Thanh NT, Colomban Ph. *J. Raman Spectrosc.* 2002; **33**: 287.
20. Liem NQ, Sagon G, Quang VX, Tan HV, Colomban Ph. *J. Raman Spectrosc.* 2000; **31**: 933.
21. Colomban Ph, March G, Mazerolles L, Karmous T, Ayed N, Ennabli A, Slim H. *J. Raman Spectrosc.* 2003; **34**: 205.
22. Colomban Ph. *J. Non-Cryst. Solids* 2003; **323**: 180.
23. Colomban Ph, Liem NQ, Sagon G, Tinh HX, Hoành TB. *J. Cult. Heritage* 2003; **4**: 187.
24. Milande V, Le Bihan L. *J. Raman Spectrosc.* 2004; **35**: 527.
25. Colomban Ph, Truong C. *J. Raman Spectrosc.* 2004; **35**: 195.
26. Colomban Ph, Sagon G, Huy LQ, Liem NQ, Mazerolles L. *Archeometry* 2004; **46**: 125.
27. Colomban Ph. In *Proceedings of CIEC 9, 9th European Interregional Conference on Ceramics, Bardonecchia, Italy*, Negro D, Montanaro L (eds), AIMAT – Polytecnicum di Torino, 2004; 6–14.
28. Wood N. *Chinese Glazes*. A&C Black: London, 1999; 27.
29. Wood N. In *Taoci No. 1. Revue Annuelle de la Société Française d'Étude de la Céramique Orientale, Actes du Colloque "Le 'Bleu et Blanc' du Proche-Orient à la Chine."* Monique Crick: Paris, 2000; 15.
30. McMillan P, Pitiou B. *J. Non-Cryst. Solids* 1982; **53**: 279.
31. Kerr R, Wood N. In *Joseph Needham: Science and Civilisation in China. Volume 5, Chemistry and Chemical Technology: Part 12 – Ceramic Technology*, Needham J, Cullen C (eds). Cambridge University Press: Cambridge, 2004; 347.
32. Gotić M, Ivanda M, Popović S, Musić S, Sekulić A, Turković A, Furić K. *J. Raman Spectrosc.* 1997; **28**: 555.
33. Huang PJ, Chang H, Yeh CT, Tsai CW. *Thermochim. Acta* 1997; **297**: 85.
34. Hu Y, Tsai HL, Huang CL. *J. Eur. Ceram. Soc.* 2003; **23**: 691.
35. Gouma PI, Mills MJ. *J. Am. Ceram. Soc.* 2001; **84**: 619.
36. Okada K, Yamamoto N, Kameshima Y, Yasumori A, Mackenzie KJD. *J. Am. Ceram. Soc.* 2001; **84**: 1591.
37. Leung PL, Yang B. *Nucl. Instrum. Methods Phys. Res. B* 1999; **155**: 452.
38. Sundius N, Steger W. 1963. In *Sung Sherds*, Palmgren N, Sundius N, Steger W (eds). Esselte: Stockholm, 1963; 375.
39. Wu J, Leung PL, Li JZ, Stokes MJ, Li MTW. *X-Ray Spectrom.* 2000; **29**: 239.
40. Yu KN, Miao JM. *Appl. Radiat. Isot.* 1997; **48**: 959.
41. Wu J, Leung PL, Li JZ, Stokes MJ, Li MTW. *X-Ray Spectrom.* 2000; **29**: 253.
42. Zhou R, Zhang F, Cheng Y. 1973; 'Technical studies on Lung-ch'uan celadons of successive dynasties,' *Chinese Translations No. 7*, Proctor P (transl). Victoria and Albert Museum in association with the Oriental Ceramic Society: London, 1977; 16–18 (originally in K'ao-ku Hsüeh-pao. 1. 1973; 1: 131–156).
43. Huffman TN, Vogel JC. *S. Afr. Arch. Bull.* 1991; **46**: 61.
44. Vogel JC. In *The Archeological Sites of Greefswald, Stratigraphy and Chronology of the Sites and a History of Investigations*, Meyer A (ed). V&R Printing Works: Pretoria, 1998; 296.
45. Hongjie L. *Ancient Chinese Pottery and Porcelain Database*. Xi'an, 1996.